LANGMUIR

pubs.acs.org/Langmuir Article

¹ Salt Effects on the Phase Behavior and Cocrystallization Kinetics of ² POCB—Water Mixtures

3 Michael Gresh-Sill, Sudesna Banerjee, Tara Y. Meyer, and Sachin S. Velankar*



Cite This: https://doi.org/10.1021/acs.langmuir.3c02428



Water-rich

liquid phase

ACCESS I

III Metrics & More

Article Recommendations

s Supporting Information

4 **ABSTRACT:** Mixtures of water with polyoxacyclobutane (POCB) have a unique 5 phase diagram which combines liquid—liquid equilibrium (LLE) at high temperatures 6 and cocrystallization of a POCB-hydrate at low temperatures. Such cocrystal hydrate 7 formation is extremely rare among polymers. We report on the effects of adding NaCl 8 salt on the phase behavior of POCB—water mixtures and the kinetics of hydrate 9 crystallization from such mixtures. Salt loadings of less than 0.1 wt % were found to 10 greatly expand the LLE region. Salt loadings of ~ 10 wt % were found to significantly 11 decrease the melting temperature of the hydrate below its ~ 37 °C value under salt-12 free conditions. The hydrate was found to be remarkably tolerant of salt and persists at 13 room temperature even when equilibrated with salt-saturated water. Salt was found to 14 slow down hydrate crystallization, and the degree of slowing was greater than that

POCB-rich liquid phase

Nac

Single-Phase POCB/water

Salt induces LLE and hydrate melting in POCB/water mixtures

Co-crystallized

solid hydrate

15 expected from the salt-induced decrease in undercooling due to melting point depression.

16 INTRODUCTION

17 Polyoxacyclobutane (POCB) is a polymer in the polyox-18 yalkylene series with the structure – $[(CH_2)_3O_-]_n$. Mixtures of 19 water with POCB show unusual phase behavior. At room 20 temperature and atmospheric pressure, POCB has a remark-21 able ability to cocrystallize with water to form a hydrate. 22 However, above the melting temperature of the hydrate, one 23 obtains a mixture in liquid-liquid equilibrium (LLE) between 24 a POCB- and a water-rich phase. Such demixing indicates 25 that—despite its apparent affinity for water in the crystalline 26 hydrate state—POCB is hydrophobic. Indeed, all other 27 polyoxyalkylenes (except poly(ethylene oxide)) are also 28 hydrophobic with very low solubility in water. This 29 combination of properties makes POCB unique: to our 30 knowledge, it is one of only two³ (possibly three⁴) polymers 31 that can form a crystalline hydrate, and the only one that also 32 phase separates from water under molten conditions. In fact, to 33 our knowledge, no other polymer is able to cocrystallize with a 34 small molecule with which it is immiscible in the liquid state.⁵ Previously, we conducted studies of the phase behavior and 36 hydrate crystallization kinetics of POCB-water mixtures. 6,7 37 Briefly, at a molecular weight of 650 g/mol, the phase diagram 38 is a union of hydrate melting behavior and LLE behavior 39 (Figure 1, discussed in detail in the Results and Discussion 40 section under liquid liquid equilibrium). Accordingly, mix-41 tures with low water content can be cooled from a 42 homogeneous liquid state to form a hydrate, and this 43 crystallization process resembles homopolymer crystallization. 44 In contrast, mixtures with a high water content are in LLE 45 prior to crystallization. Thus, hydrate formation involves 46 interfacial mass transport and is, therefore, sensitive to mixing 47 conditions.

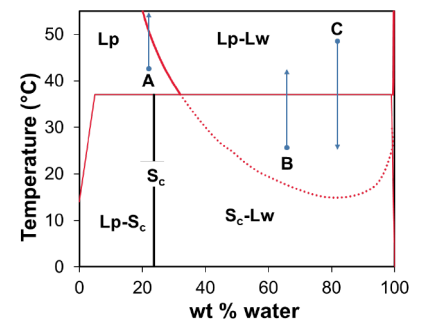


Figure 1. Phase diagram for POCB 650 and water without salt.² The solid black line labeled Sc indicates the composition of the solid hydrate. The solid red curve indicates the liquid—liquid coexistence between the polymer-rich (Lp) and water-rich (Lw) phases, whereas the horizontal red line is the melting point of the hydrate. The dotted red line indicates a metastable portion of the liquid—liquid coexistence curve. The blue arrows indicate the trajectories used for the measurements of interest in this study. (A) Heating a single-phase mixture to locate the cloud point (liquid—liquid equilibrium section).

(B) Heating a hydrate—liquid mixture to measure the melting point (melting point section). (C) Cooling a two-phase mixture in LLE to measure the crystallization kinetics (crystallization kinetics section). This diagram is not strictly correct, as discussed in the liquid—liquid equilibria section.

Received: August 21, 2023 Revised: January 2, 2024 Accepted: January 5, 2024



POCB-hydrate formation has many potential applications 49 including improving the nonvolatile memory storage capa-50 bilities of carbon nanotube devices, drug delivery or other 51 biomedical applications, 9,10 water purification, 11 materials with 52 high proton and ion conductivity for membrane applica-53 tions, 12,13 and stimuli-responsive materials. 14 Ionic solutes are 54 expected to be present in virtually all of these applications. The 55 effect of ionic solutes on the phase behavior and hydrate 56 crystallization kinetics of POCB/water mixtures is unknown 57 and the subject of this paper. Salt is known to affect the 58 solubility of polymers through the Hofmeister effect. 15 Thus, 59 we anticipate that salt promotes the immiscibility of POCB 60 and water, and indeed this was noted previously 16 as discussed 61 further below. Additionally, any solute can reduce the melting 62 point of a crystal. Thus, salt is expected to affect the phase 63 boundaries of both the LLE and solid-liquid equilibrium in 64 the POCB-water mixtures. These changes in the phase 65 behavior are also likely to affect the crystallization kinetics. For 66 example, melting point depression of the hydrate would reduce 67 the undercooling (at any specified crystallization temperature), 68 and hence, the addition of salt would also slow crystallization. The goal of this paper is to measure these effects quantitatively. We are aware of only one previous publication of salt effects 71 on POCB/water mixtures. 16 Lee et al. showed that salt-free 72 POCB/water mixtures that were transparent, homogeneous 73 mixtures at room temperature reached a cloud point (i.e., demixed) upon heating, and further that the cloud point temperature reduced upon the addition of NaCl. This research 76 was conducted at a POCB molecular weight of 250 g/mol¹⁶ and did not mention hydrate formation at all. Indeed, our experiments with a similarly low molecular weight show that the hydrate does not form readily. The research in this paper 80 will focus on the effects of NaCl as the salt but will use a MW 81 of 650 g/mol of POCB at which hydrate crystallization and 82 LLE are coupled with each other. It is this coupling that makes 83 this system unique, and there have been no previous studies of 84 salt effects on any similar polymer-water mixture.

The salt-induced demixing seen in POCB/water mixtures previously 16 and in this paper is common across a variety of water-soluble polymers, wherein the solubility of the polymer in water reduces with increasing salt content. These include polymers of the polyoxyalkene series, such as short chain polyoxymethylene (POM), poly(ethylene oxide) (PEO), poly(propylene oxide) (PPO), and POCB, as well as other polymers such as polyvinylpyrrolidone (PVP), poly(N-93 isopropylacrylamide) (PNIPAM), or poly(2-oxazoline) (POX). Similar salt effects are also seen in other aqueous nonionic polymer mixtures such as dextran—polyvinylpyrrolidone, dextran—poly(vinyl alcohol), dextran—ficoll, and dextran—PEG. These aqueous systems have been known since the late 1800s and have been studied for their use in biological separations since Albertsson's group pioneered the practice in the 1950s. 15,26

In contrast to the well-established literature on salt effects on 102 LLE in water—polymer mixtures, we are unaware of any studies 103 on the effects of salt on crystallization of polymer hydrates. 104 There are, however, limited studies of salt effects on 105 homopolymer crystallization in the absence of water. Salt can 106 significantly slow down the kinetics of crystallization, 27–29 107 which is at least partially attributed to the reduction in the 108 equilibrium melting temperature of the homopolymer, and 109 thereby a reduction of undercooling. Any reduction beyond 110 the decrease in undercooling may be attributable to more

complex effects such as change in surface energy at the 111 crystal—amorphous interface or transport limitations to 112 crystallization. Incidentally, outside the polymer science 113 literature, salt effects on gas hydrates or other small-molecule 114 clathrate hydrates are well studied. Salt is known to reduce the 115 melting temperature of the hydrate, as well as slow down 116 crystallization. However, these clathrate hydrates are very 117 different: they have a water-cage structure (vs the intercalated 118 structure of POCB-hydrate); the water content of gas hydrates 119 is far higher than in POCB-hydrate; and the growth 120 mechanism and habit of gas hydrates are entirely distinct 121 from those for POCB hydrate.

■ RESULTS AND DISCUSSION

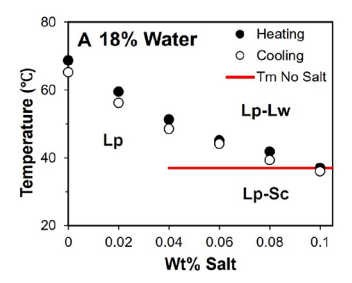
The results section is organized into two parts. The Salt Effects 124 on Phase Behavior section describes the effects of salt on the 125 phase diagram, both on how salt affects LLE (as judged by 126 cloud point measurements, "Liquid Liquid Equilibria" see 127 tion), and the melting temperature of the hydrate. In both of 128 these cases, we report changes in phase behavior at a fixed 129 polymer fraction while varying the salt content and fixed salt 130 content while varying the polymer fraction. The Melting Point 131 of the hydrate section describes the effect of salt on the kinetics 132 of hydrate crystallization. Details of the experimental methods 133 and data analysis are given at the end of the paper.

123

Salt Effects on Phase Behavior. Liquid—Liquid Equi- 135 libria. As shown in Figure 1, at the molecular weight of 650 g/ 136 mol, in the absence of salt, the LLE behavior had the following 137 characteristics. Above 37 °C (the melting temperature of the 138 hydrate), the mixtures are in LLE between water-rich and 139 POCB-rich phases. The miscibility gap (i.e., the difference 140 between the compositions of the water-rich and the POCB- 141 rich phases) widens at higher temperatures, suggesting that the 142 LLE curve has a lower-consolute solution temperature 143 (LCST). Below 37 °C, while mixtures may remain in LLE 144 for short periods, the hydrate forms eventually. This portion of 145 the LLE curve is metastable, and we were not able to quantify 146 it fully.

It must be noted that Figure 1 is schematic, and hence, not 148 strictly correct. First, at very low polymer (or very low water) 149 content, there must be a small region of melting point 150 depression of ice (or of pure solid POCB). These regions 151 could not be explored experimentally since the corresponding 152 polymer or water contents are too low. Second, the hydrate 153 melting points did not show measurable changes with 154 composition, and hence, the hydrate melting line is shown to 155 be horizontal. While this is correct for the three-phase (Lp- 156 Lc-Sc) coexistence region, it may not be true for the Lp-Sc 157 coexistence since the hydrate melting point must be depressed 158 for compositions near the crystal composition (23.6 wt % 159 water). Evidently, this melting point depression is too small to 160 be measured in our experiment. Third, at low water content, 161 crystallization takes a long time and thermodynamic 162 equilibrium may not be maintained. Nevertheless, the phase 163 diagram in Figure 1 is consistent with our experiments and 164 suitable for guiding this paper.

Turning now to the effects of salt, a first set of experiments $_{166}$ was conducted at fixed water content (18 wt %) to gauge the $_{167}$ amount of salt needed to induce a noticeable depression in the $_{168}$ cloud point. Figure 2A shows the cloud point for samples with $_{169}$ fz 0.0 to 0.1 wt % salt. The cloud point is found to reduce from $_{170}$ around $_{67}$ °C for the salt-free mixture to around $_{36}$ °C at 0.1% $_{171}$ salt. Above 0.1% salt, the cloud points are below the melting $_{172}$



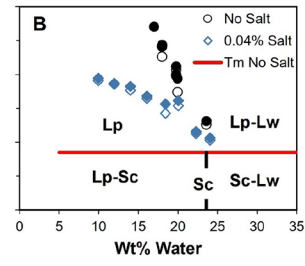


Figure 2. Cloud points for POCB/water/salt mixtures. (A) Cloud points for samples with 18% water vs salt content. Below these cloud points, the mixtures are single-phase liquids, whereas two liquid phases (lp and lw) exist above the cloud points. (B) Cloud points for samples without salt and with 0.04% salt at various water contents. Samples are single-phase below the black circles for the salt-free samples and below the blue diamonds at 0.04% salt. The vertical black line labeled Sc indicates the composition of the POCB-water hydrate. In both graphs, the open symbols represent cloud points measured during cooling, and the closed symbols represent cloud points measured during heating. In both graphs, the solid red line is the melting point of the hydrate, which is nearly independent of salt content (see text) and water content. In part B, the red line does not extend below 5% water because slow crystallization makes it difficult to study hydrate melting. A single pair of heating-cooling points is shown in each graph. Yet, the reproducibility of two independently prepared samples is better than the difference between the heatingcooling pair shown.

173 temperature of the hydrate; therefore, mixtures in LLE must 174 eventually crystallize. While nonequilibrium cloud points can 175 be measured, in the present case, hydrate crystallization was 176 too rapid to allow such quantification.

The water-rich branch of the cloud point curve was not quantified in this research. Previously we noted that in the absence of salt, the addition of even 1% POCB (MW 650 g/ 180 mol) to pure water brings the mixture into the LLE. Thus, the boundary of the LLE region extends to nearly pure water, making it difficult to quantify precisely. This remains true with the addition of salt.

The magnitude of cloud point depression observed here is 185 far larger than in Lee et al. ¹⁶ who found that a similar 30 °C 186 drop required a salt loading of 5.0 wt % vs less than 0.1 wt % in 187 Figure 2A. This difference may be attributable to the 188 differences in MW between our samples (650 g/mol) vs Lee 189 (250 g/mol). Indeed, in solutions of other polymers such as 190 PEO, PVP, and PNIPAM, ^{18,21–23} the magnitude of cloud point 191 depression with added salt is known to increase with MW.

Based on the results of Figure 2A, a second set of 193 experiments was then conducted at a fixed salt content of 194 0.04 wt %, varying the water content from 10 to 20 wt %. 195 Figure 2B shows that the magnitude of cloud point reduction is 196 more severe as the water content reduces. This latter 197 observation may be rationalized as follows.

The common explanation for the salt effect on cloud point depression is a result of polymer—ion interactions and competition for hydration. 18,19,26,31–33 Qualitatively, the ions avoid association with the polymer and instead prefer to associate with water. This reduces the level of hydration of the polymer, eventually inducing the formation of a separate, polymer-rich liquid phase. Indeed, this effect is not limited to polymers; homogeneous mixtures of water with organic solvents can be induced to phase separate upon adding solvents. As the water content reduces while the salt loading is held fixed, the amount of water available for hydrating the

polymer reduces steeply, thus, making LLE more favorable. 209 Therefore, samples with lower water content show a larger 210 magnitude of cloud point depression in Figure 2B.

Finally, a complete description of LLE also requires 212 examination of the partitioning of the salt into the two 213 coexisting phases. We presume that salt would preferentially 214 partition into the water-rich phase, with very little being 215 present in the POCB-rich phase. This was verified in a single 216 experiment (see ESI), which establishes that the POCB-rich 217 phase can dissolve at most 0.01% salt at 40 °C, even when the 218 aqueous phase is saturated saltwater. When the aqueous phase 219 is much more diluted, e.g., as in Figure 2, we presume that the 220 POCB-rich phase has even lower amounts of salt.

Melting Point. Preliminary experiments showed that the 222 mixtures from the previous section (with up to 0.1% salt) 223 induced negligible melting point depression; several percent 224 salts were needed to reduce the hydrate melting point 225 measurably. Accordingly, separate samples were made at 226 higher salt contents.

Similar to the previous section, initial experiments were 228 conducted at a fixed water loading to identify the salt content 229 needed to see a measurable decrease in the melting 230 temperature. Similar to previous experiments,² we first cooled 231 the mixtures (which are initially in LLE) in vials to create 232 hydrates, and then gradually heated them under microscope to 233 observe the highest temperature at which hydrate crystals still 234 persist. Figure S1 shows exemplary images during the melting 235 process. These experiments were conducted at 30% POCB, i.e., 236 a much higher water content than in Figure 2 because at 30% 237 POCB, mixtures develop a waxy solid-like consistency during 238 crystallization, making it easy to transfer from the vial to the 239 microscope stage. In contrast, samples with much higher or 240 lower water content undergo large-scale phase separation and 241 sedimentation; and hence, the composition of the sample 242 transferred to the microscope deviates from the original 243 sample. Samples of fixed POCB content (30 wt %) were 244 prepared with salt loadings varying from 0.0 to 15.0 wt %. 245 Their melting points, $T_{\rm m}$ (Figure 3A): were found to reduce by 246 f3 several degrees over the range of salt content examined.

It is interesting to consider the state of the mixtures in 248 Figure 3A prior to melting. We define $m_{\rm s}$, $m_{\rm p}$, and $m_{\rm w}$ as the 249 weight fractions of the salt, polymer, and water in the overall 250 mixture and take a unit mass of the mixture as basis. If χ is the 251 fraction of the POCB that crystallizes to form hydrate, then the 252

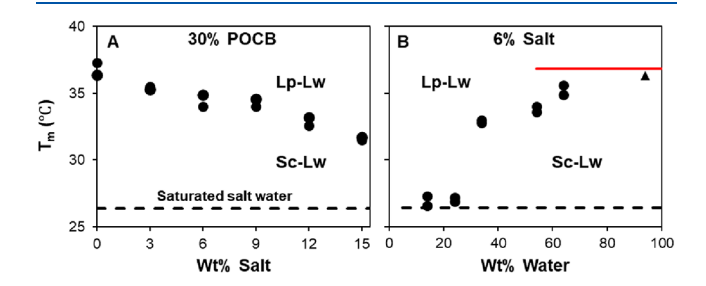


Figure 3. (A) The hydrate melting temperature obtained from optical microscopy for varying salt contents and fixed POCB loading of 30 wt %. (B) Melting temperature for varying water contents with a fixed salt loading of 6 wt %. The solid red line indicates the melting point for hydrate crystals with no salt present. The dashed line indicates the melting temperature of hydrate crystals in equilibrium with saturated salt water. The black triangle denotes a dilute POCB sample in 6% saltwater.

253 mass of water consumed in hydrate formation is $0.31\chi m_{\rm p}$ per 254 unit mass of mixture (since the hydrate has a POCB:water 255 ratio of 1:0.31). The salt fraction in the water-rich (Lw) phase 256 is now

$$m_{\rm s}^{\rm Lw} = \frac{m_{\rm s}}{1 - m_{\rm p}(1 + 0.31\chi)} \tag{1}$$

The above assumes that the POCB-rich phase is nearly pure, 258 259 the water-rich phase has negligible dissolved POCB, and (as 260 discussed in the Melting point of hydrate section) all the salt 261 partitions into the water-rich phase. For the highest salt 262 loading in Figure 3A, m_s = 0.15 and m_p = 0.3. If we assume full crystallization, $\chi = 1.0$, eq 1 gives $m_s^{Lw} = 0.247$. This last number is close to the weight fraction of salt in salt-saturated water (roughly 0.27), i.e., as per this calculation this fully crystallized mixture would have an aqueous phase that is nearly saturated with salt. The above estimate of the salt fraction of 268 0.247 is an upper bound, since it assumes full crystallization of 269 POCB, while polymers never crystallize to their full extent. In 270 fact, we noted previously, 6,7 that in the absence of salt, the 271 volume change of crystallization was approximately half of that 272 expected for full hydrate crystallization. Thus, if we take $\chi =$ 0.5, eq 1 gives $m_s^{\text{Lw}} = 0.230$, which is still relatively close to full saturation. This calculation raises an interesting question: can the hydrate coexists with saturated water, and if so, what is the 276 melting temperature of the hydrate in equilibrium with saltsaturated water? 277

To address this, a separate experiment was conducted. A small amount of POCB was added to pure water to precipitate the hydrate crystals. A small quantity of the crystals was transferred to a vial of salt water with excess salt (i.e., the aqueous phase is salt-saturated water), which was then heated gradually until the crystals melted. The corresponding Figure 3, serves as a lower bound for the melting point in Figure 3, and corresponds to four-phase equilibrium between hydrate, salt crystals, a POCB-rich liquid phase, and saturated lass salt water (with very little POCB). It is noteworthy that this temperature exceeds room temperature, i.e., the hydrate is sufficiently salt-tolerant that does not melt even when equilibrated with salt-saturated water at room temperature.

Finally, Figure 3B shows the dependence of melting point on 293 the composition at a fixed salt content of 6 wt %. The point 294 marked with a black triangle represents an experiment in which 295 a small amount of hydrate crystal particles was placed in 6% 296 saltwater and then melted. The corresponding hydrate melting 297 point of $T_{\rm m}$ = 36.3 °C shows no significant melting point 298 depression as compared to the melting of a hydrate in 299 equilibrium with pure water. With decreasing overall water 300 content, the melting point reduces precipitously once the 301 overall water loading in the mixture decreases below 40 wt %, 302 and levels off at about 27 °C, close to the value for the hydrate 303 in equilibrium with salt-saturated water. This may be 304 rationalized from eq 1, once again taking $\chi = 0.5$ for the 305 following example calculations. The overall water loading of 306 34% in Figure 3B corresponds to $m_s = 0.06$, $m_p = 0.6$, and $m_w = 0.6$ $_{307}$ 0.34. For this composition, eq 1 gives $m_{\rm s}^{\rm Lw} = 0.195$, thus, at 308 34% overall water, with crystallization of half of the POCB, the 309 aqueous phase is still well below the saturation point. However, 310 at an overall water loading of 24%, the mixture compositions 311 are $m_s = 0.06$, $m_p = 0.7$, and $m_w = 0.24$. For this composition, eq 1 gives $m_{\rm s}^{\rm Lw}=0.31$, corresponding to a supersaturated salt $_{312}$ solution. Therefore, the steep drop in $T_{\rm m}$ below 40% water and $_{313}$ the plateau around $T_{\rm m}=27$ °C at low water loading are $_{314}$ consistent with the aqueous phase first approaching saturation $_{315}$ and then becoming supersaturated. Indeed, salt crystals were $_{316}$ observed in samples with 70 and 80 wt % POCB prior to $_{317}$ melting. Since, the water-rich phase is salt-saturated, it is $_{318}$ unsurprising that $T_{\rm m}$ shows a plateau at a value similar to that $_{319}$ of the hydrate crystals placed into a vial of salt-saturated water. $_{320}$

Crystallization Kinetics. The study of phase behavior 321 from the previous section guides our experiments on hydrate 322 crystallization kinetics in two important ways. First, Figure 3 323 shows that the salt lowers the equilibrium melting temperature. 324 Thus, at any specified crystallization temperature, T_c , 325 increasing salt loading reduces the undercooling $(T_{\rm m}-T_{\rm c})$ 326 and is expected to slow down crystallization kinetics. The 327 second is that in mixtures containing over 0.1% salt, above $T_{\rm m}$, 328 LLE prevails at almost all POCB:water ratios (Figure 2). Thus, 329 prior to crystallization, the mixture is almost always in LLE, 330 and hence, three phases (two liquid, and the solid hydrate) are 331 present during crystallization.^{6,7} Moreover, in general, neither 332 of the two liquid phases coexisting during crystallization has 333 the same composition as the hydrate. Instead, the water-rich 334 phase is diluted in POCB, whereas the polymer-rich phase is 335 diluted in water; the latter, especially, may change with salt 336 content and crystallization temperature. Therefore, in general, 337 hydrate crystallization may involve interfacial mass transport 338 and hence is expected to depend on the mixing conditions. 339 Accordingly, differential scanning calorimetry, the common 340 method for studying the crystallization kinetics of polymers, 341 cannot be used. Instead, we examined the hydrate crystal- 342 lization kinetics by dilatometry, stirring the dilatometer flasks 343 continuously with magnetic stir bars to avoid density-based 344 separation. This is possible only at relatively low viscosity, 345 necessitating a relatively low POCB content. Accordingly, our 346 kinetic study was restricted to POCB-water mixtures with a 347 low POCB content of 20 wt %. The kinetics data on salt-free 348 samples were discussed comprehensively in a separate study by 349 Banerjee et al.

Mixtures with 20 wt % POCB, salt loading ranging from 0.0 $_{351}$ to 7 wt %, and the remainder water were prepared in a $_{352}$ dilatometer with a magnetic stirrer. For each experiment, $_{353}$ samples were held above their melting point in a hot bath at 48 $_{354}$ °C and then transferred to a second bath held at a fixed $_{355}$ crystallization temperature $_{7c}$. Volume changes were measured $_{356}$ by quantitative video analysis over the course of 3–6 h. 2–4 $_{357}$ samples were prepared at each individual composition, and $_{358}$ each sample was crystallized isothermally at various values of $_{359}$ $_{7c}$

As described previously, 6,7 upon cooling to T_{c} , two forms of 361 volume change were observed. Within the first few minutes, 362 the volume decreased due to thermal contraction as the 363 samples cooled from 48 °C to T_{c} . Over a longer period, there 364 was a further volume decrease due to crystallization. This latter 365 volume decrease occurred more quickly at lower crystallization 366 temperatures, and hence at sufficiently low T_{c} values, 367 crystallization started even before the thermal contraction 368 was completed. Such fast crystallization is no longer isothermal 369 and was not analyzed. The volume change associated with 370 crystallization was obtained by subtracting the volume change 371 due to thermal contraction from the total volume change 4 shows examples of the specific volume change due to 373 feligure 4 shows examples of the specific volume change due to

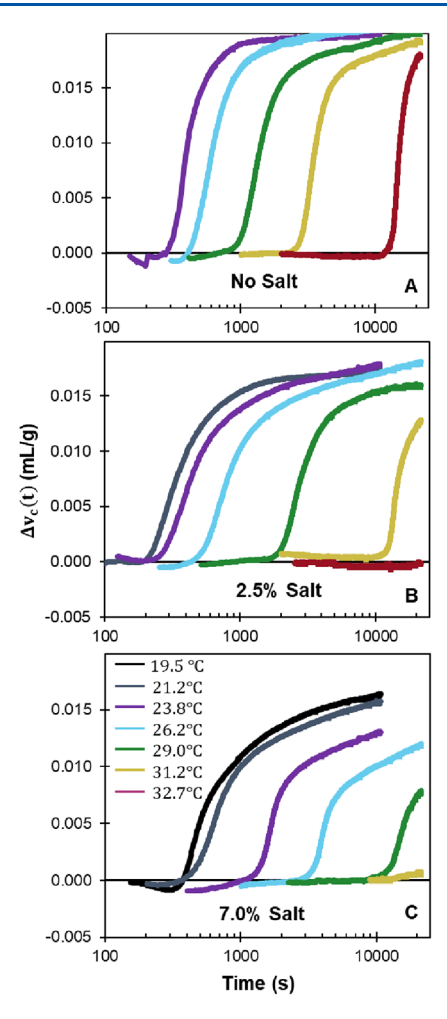


Figure 4. Time-evolution of specific volume change during crystallization at various temperatures. All samples have 20.0 wt % POCB, and salt weight percentages noted at the bottom of each figure.

374 crystallization, $\Delta v_{\rm c}(t)$, for samples with 20 wt % POCB, 375 without salt, with 2.5 wt % salt, and with 7.0 wt % salt. Other 376 intermediate values of salt loadings are shown in Figure S3. As 377 previously described, even though crystallization shrinks the 378 volume of the mixture, $\Delta v_{\rm c}$ is shown as a positive quantity.

Each crystallization trial follows a similar pattern of an initial small latent period without significant crystallization, followed by small rapid crystallization and an eventual plateau at some final value. The duration of the initial latent period grew with increasing small content; compare for instance the time at which crystallization starts at 29 °C in Figure 4A (roughly 1000 s) small value. This trend points toward salt having an inhibiting effect on the cocrystallization kinetics of POCB hydrate. An analogous salt effect was described by Bianchi²⁷ small value. The presence of salt inhibited the crystallization of small poly(caproamide).

As previously, we seek to quantify the crystallization 391 behavior in terms of two parameters: the value of Δv_c at 392 long times $\Delta v_c^{\text{final}}$, and the time needed to reach a specified 393 value of Δv_c . To estimate $\Delta v_c^{\text{final}}$, we plotted the value of Δv_c at 394 $t=10^4$ s (selected arbitrarily) for each experiment. Figure S4 395 shows that this value increases with decreasing temperature T_c , 396 and then it shows a plateau. This suggests that at sufficiently 397 low temperature crystallization is complete by 10^4 s. $\Delta v_c^{\text{final}}$ was

taken as the average of $\Delta \nu_c$ values from the six lowest 398 temperatures available for each composition. Figure 5 shows 399 fS that the $\Delta \nu_c^{\rm final}$ does not change any systematic way with salt $_{400}$ content.

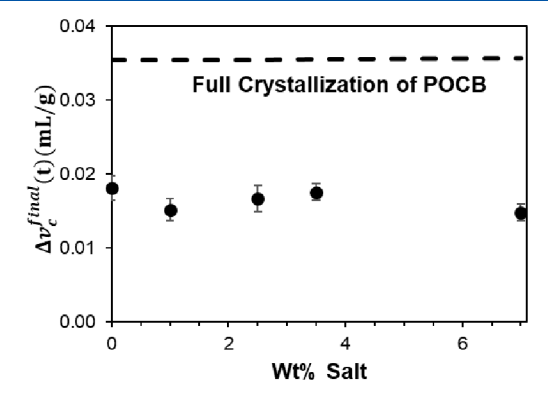


Figure 5. Average specific volume change at long crystallization times for samples with 20 wt % POCB. The dotted line indicates the theoretical maximum value predicted by eq 2.

A theoretical maximum volume change, $\Delta \nu_{\overline{Q}}^{max}$ (assuming all 402 POCB is consumed to form hydrate), can be estimated as 403

$$\Delta v_{\rm c}^{\rm max} = \left(\frac{m_{\rm w} + m_{\rm s}}{\rho_{\rm aq,i}} + \frac{m_{\rm p}}{\rho_{\rm p}}\right) - \left(\frac{\frac{m_{\rm POCB}}{0.764}}{\rho_{\rm c}} + \frac{1 - \frac{m_{\rm POCB}}{0.764}}{\rho_{\rm aq,f}}\right)$$
(2) 40

where $ho_{
m aq,\it ij}$ $ho_{
m aq,\it fj}$ $ho_{
m POCB}$, and $ho_{
m c}$ are the densities of the aqueous 405 phase before crystallization, the aqueous phase after crystal- 406 lization, POCB, and the hydrate crystal respectively, and 0.764 407 is the weight fraction of POCB in the crystal. The term in the 408 first brackets is the sum of the specific volume of the saltwater 409 and liquid POCB, which are assumed to be completely 410 immiscible. The term in the second brackets is the sum of the 411 specific volumes of the hydrate crystal and the uncrystallized 412 saltwater. The density of the crystal phase is ρ_c = 1.176 g/mL 413 (based upon dimensions of the unit cell, 34 and the density of 414 POCB is $\rho_{POCB} = 1.02$ g/mL. The density of the saltwater 415 phase is calculated for each composition based upon the model 416 provided by Simion³⁵ by assuming that all the salt is in the 417 aqueous phase both before and after crystallization. Further all 418 densities are assumed to be independent of temperature. The 419 prediction of eq 2 (dashed line in Figure 5) is found to be 420 nearly independent of salt content (in effect, $ho_{
m aq,i}$ and $ho_{
m aq,f}$ only 421 weakly depends on salt content).

The predicted value is found to be nearly twice of the 423 measured values of $\Delta \nu^{\rm final}$ suggesting that only roughly 50% of 424 the POCB actually crystallizes at any given salt content. This 425 value of 50% crystallization is similar to that estimated from 426 previous experiments in which the hydrate crystallized from a 427 homogeneous liquid phase with an excess POCB. Yet, it 428 should be noted that this conclusion of 50% crystallization 429 depends on the estimated crystal phase density. Even a few 430 percent error in the published values of unit cell dimensions 431 change the $\rho_{\rm c}$ value, and hence the value of $\Delta \nu_{\rm c}^{\rm max}$ 432 significantly. 6

Next, we turned to the effect of salt on the crystallization ⁴³⁴ rate. As in our previous studies ^{6,7} to quantify the kinetics, from ⁴³⁵ each $\Delta v_c(t)$ curve, we identified the time τ at which the volume ⁴³⁶ change reached 0.005 mL/g (chosen arbitrarily), i.e., $\Delta v_c(t = 437)$

438 τ) = 0.005 mL/g. This time τ provides a single number to 439 compare the kinetic data at all salt contents. Figure 6 shows τ

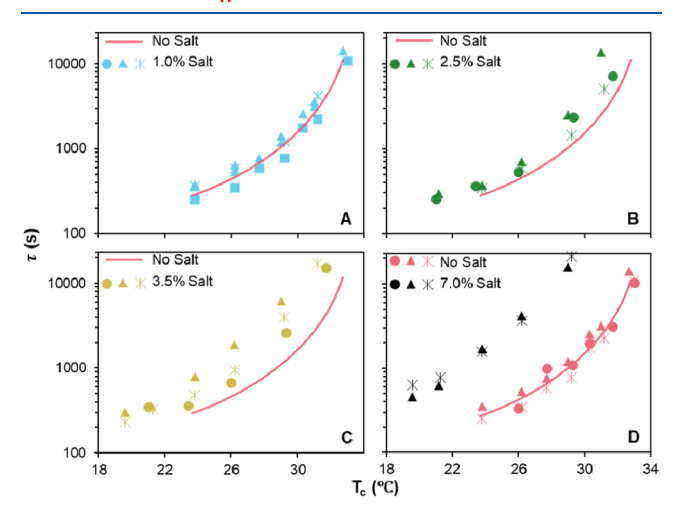


Figure 6. Time for $\Delta \nu_c = 0.005$ mL/g at various crystallization temperatures. All samples have 20 wt % POCB, with varying salt contents. The pink data in D corresponds to the salt-free sample which is 'reproduced with permission from Ref.,⁷ copyright [2023][Elsevier-polymer]' and the pink line in A, B and C are a guide to the eye. Different symbols in each graph represent distinct samples of the same composition.

440 versus crystallization temperature $T_{\rm c}$. The corresponding salt-441 free data are shown only in Figure 6D, but the solid pink line 442 passing through the salt-free data is shown in Figures 6A-D for 443 comparison. In general, increasing salt content increases τ , i.e., 444 slows down crystallization, although the effect is modest below 445 3 wt % salt.

As mentioned at the beginning of this section, the salt-447 induced melting point depression reduces the undercooling 448 $\Delta T = (T_{\rm m} - T_{\rm c})$, and hence, it is expected to slow 449 crystallization. To quantify the extent of this effect, we must 450 therefore compare τ values at fixed undercooling, rather than at 451 fixed $T_{\rm c}$. The well-established approach for doing so is the 452 Hoffman–Lauritzen theory which relates the kinetics of 453 crystallization to the free energy of secondary nucleation on 454 the face of the growing crystal. It predicts crystallization rate as

crystallization rate
$$\propto \exp\left(-B\frac{T_{\rm m}}{T_{\rm c}\Delta T}\right)$$
 (4)

Note that the quantity $T_{\rm m}/T_{\rm c}$ is close to 1 in our case, thus to a first approximation, the right-hand side depends on ΔT 458 alone. Accordingly, eq 4 accounts for the changes in 459 undercooling due to melting point depression; if that is the 460 only factor by which salt affects crystallization kinetics, then 461 one would expect data at all salt contents to collapse onto a 462 single line. That would suggest that the only effect of salt is to 463 slow down the secondary nucleation necessary for crystal 464 growth.

Accordingly, with τ^{-1} as a measure of the crystallization rate, and Figure 7 plots $ln(\tau^{-1})$ vs $T_{\rm m}/T_{\rm m}\Delta T$. While the number of 467 points for each sample are small, the data do appear 468 approximately linear, consistent with eq 4, i.e., the Hoff-469 man—Lauritzen model can represent the data at least 470 approximately. A detailed discussion of the salt-free data was 471 presented previously; here we only focus on the effects of salt. 472 Even though data at the different salt contents do move closer

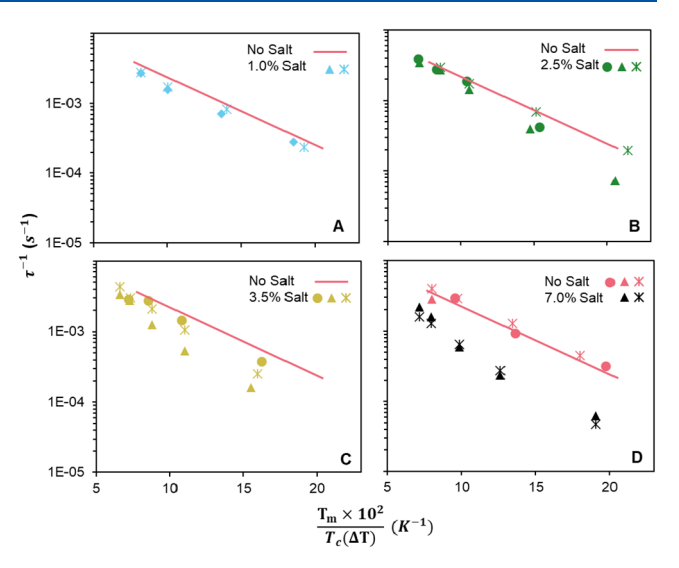


Figure 7. Time for $\Delta \nu_c = 0.005$ mL/g for various salt contents in the form of a Hoffman–Lauritzen plot. Different symbols in each graph represent a distinct sample of the same composition. The pink data in D corresponds to the salt-free sample which is 'reproduced with permission from Ref.,⁷ copyright [2023][Elsevier-polymer].' The pink straight line corresponds to eq 4 for the salt-free data and is reproduced in A-C as a reference.

together than in Figure 6, data for the various salt samples 473 remain distinctly below the salt-free line. These results indicate 474 that the salt effects on undercooling can account for only a part 475 of the slowing of the crystallization kinetics. We emphasize that 476 this last conclusion does not rely on the validity of the 477 Hoffman—Lauritzen model. The effect of salt-induced melting 478 point depression can be judged without guidance from Eq 4: 479 Simply plotting the results of Figure 6 with ΔT on the x-axis 480 shows that, even when compared at fixed undercooling, salt 481 slows hydrate crystallization. Finally, the samples at 2.5 and 482 3.5% show a large degree of sample-to-sample variability with 483 some behaving similar to the sample without salt, and some to 484 the sample with 7 wt % salt. It is possible that the mechanism 485 of crystallization changes across this concentration range.

Figure 7 also shows a distinct increase in the temperature- 487 dependence of the crystallization kinetics with increasing salt 488 content. For homopolymers, a decrease in slope of the 489 crystallization kinetics vs $T_{
m m}/T_{
m m}\Delta T$ indicates a decrease in the 490 surface energy at the crystal-melt interface as per the 491 Hoffman-Lauritzen model.³⁶ Accordingly, Figure 7 indicates 492 that increasing salt concentration reduces the surface energy. 493 In the current situation, however, hydrate crystallization occurs 494 from a mixture of polymer, salt, and water. For a homopolymer 495 crystallizing from a mixture, there is an additional contribution 496 to the slope that comes from the concentration of the 497 polymer.³⁷ Although we keep the polymer loading fixed at 20 498 wt % in all samples, the compositions of the coexisting liquid 499 phases may change with salt content and may in turn affect the 500 temperature-dependence. Thus, it is difficult to conclusively 501 pin down the reason underlying the increasing temperature- 502 sensitivity of the crystallization kinetics with increasing salt 503

As in Banerjee et al., 7 we also considered an alternate sos method to quantify kinetics which is based on the induction sof time, i.e., the time up to which Δv_c remains nearly zero (see sor short time behavior in Figure 5). This induction time, $t_{\rm ind}$, has sos been regarded as the time for primary nucleation 38 and serves so

455

510 as another measure of crystallization kinetics. Analysis of data 511 based on the induction time (see ESI) gives conclusions that 512 are essentially identical to those based on analysis using the 513 time scale τ .

514 SUMMARY AND CONCLUSIONS

515 To summarize, inorganic salts are well known to induce 516 liquid—liquid separation in aqueous solutions of many water-517 soluble polymers. This paper examines the effects of adding 518 salt to mixtures of polyoxacyclobutane (POCB) and water. 519 POCB has the rare ability to cocrystallize with water to form a 520 hydrate, one of only two or three polymers that can do so. 521 Further, above the melting temperature of the hydrate, 522 mixtures of POCB and water can exist in liquid—liquid 523 equilibrium (LLE). This combination of immiscibility in the 524 liquid phase and cocrystallization at low temperature gives 525 POCB—water mixtures a phase diagram that is distinct from all 526 other polymer—solvent pairs. Here, we report on the effect of 527 adding NaCl salt to the phase diagram of POCB—water 528 mixtures and to the kinetics of hydrate crystallization.

529 The central results of this paper are as follows.

1. Even small loadings of salt (less than 0.1 wt %) can significantly expand the composition range within which LLE sale appears, i.e., there is a salting-out effect similar to other aqueous polymer solutions. The expansion of LLE, as judged by lowering of the cloud point temperature, is especially severe sale at low water content. This suggests that the reason why salt drives LLE is that by demixing of the polymer and water and partitioning into the aqueous phase, the salt can avoid sale sassociation with the polymer.

2. Much larger salt loadings (\sim 10 wt %) reduce the melting temperature of the hydrate.

3. The hydrate is remarkably salt-tolerant and can coexist even with salt-saturated water. Accordingly, the lowest melting point of the hydrate (i.e., the greatest melting point depression of the hydrate) corresponds to a four-phase equilibrium between a POCB-rich liquid phase, a water-rich liquid phase, solid hydrate, and solid NaCl. The corresponding four-phase equilibrium temperature is 26 °C, just above room tempersature.

4. Since salt greatly shrinks the homogeneous liquid region, 550 in POCB—water—salt mixtures, hydrate crystallization starts 551 from the LLE state at almost all compositions. Bulk 552 crystallization experiments (conducted with continuous 553 stirring to avoid layering of the two liquids) show that salt 554 decreases the crystallization rate. The decrease in rate is 555 modest for ~1 wt % salt loading but approaches 10x at the 556 highest loading (7% salt) examined. Some, but not all, of the 557 slowing of hydrate crystallization can be explained by the 558 melting point depression, i.e., the fact that at any given 559 crystallization temperature, salt-containing samples are at lower 560 undercooling.

To the best of our knowledge, the latter two items are the first report of any salt effect on the phase behavior or crystallization kinetics of a polymer hydrate cocrystal.

Overall, the effect of salt on the LLE behavior of POCB—565 water mixtures is similar to that of other aqueous polymer 566 solutions. The effect of salt on the hydrate melting point is 567 qualitatively similar to the melting point depression of any 568 crystal equilibrating with a solute. Finally, the fact that salt 569 slows the hydrate crystallization even when compared to fixed 570 undercooling suggests that salt may have additional interfacial

effects that slow crystallization beyond what may be expected 571 from melting point depression alone. 572

573

EXPERIMENTAL

Materials. Polyoxacyclobutane was obtained from DuPont under 574 the trade name Cerenol. The experiments used POCB with a number- 575 average molecular weight of 650 g/mol, as reported by the 576 manufacturer. The glassware used in the dilatometry experiments 577 was prepared in a glass shop at the University of Pittsburgh. As even 578 small salt impurities were found to significantly alter cloud-point 579 results, Millipore water was used in all samples.

Cloud Point Methods. POCB—water—salt mixtures (roughly 3 g 581 total) were weighed into small glass vials. The vial lid was closed and 582 sealed with a silicone sealant to prevent any water loss due to 583 evaporation. The samples were immersed in a water bath with the 584 temperature controlled by a hot plate. The bath temperature was 585 gradually raised until sample cloudiness became visually apparent and 586 then lowered to verify the disappearance of cloudiness. For these 587 experiments, it was necessary for the entire vial to be immersed in a 588 water bath. If any portion of the vial, e.g., the cap, was exposed to 589 cooler air during the experiment, condensation of water on the cooler 590 surface confounded the results.

Melting Point Methods. POCB—water—salt mixtures were 592 weighed into small glass vials and allowed to crystallize at room 593 temperature over many days. A small quantity of the resulting 594 hydrate—liquid mixture was then placed into a polystyrene well plate 595 and flattened. This well plate was placed under a microscope in a 596 temperature-controlled stage and heated in 2 °C increments starting 597 from 22 °C. The temperature at which the hydrate crystals were no 598 longer visible was taken as the melting point temperature for that 599 sample.

Crystallization Measurement Methods. POCB-water-salt 601 mixtures (roughly 1 g in total) were weighed into round-bottom 602 flasks. A magnetic stir bar was added to all samples. The samples were 603 then covered with mineral oil, and the flasks were joined to a capillary 604 stem and sealed with parafilm. The samples were heated to 48 $^{\circ}\text{C}$ to $_{605}$ ensure all hydrate crystals were melted and then cooled rapidly in a 606 water bath set to the desired crystallization temperature. All the 607 graphs and the data analysis use the true temperature that was 608 continuously read off of a calibrated digital thermometer immersed in 609 the water bath. Typically, the temperature during any single 610 experiment varied no more than ±0.1 °C. The samples were stirred 611 continuously during this process (see the next paragraph). The 612 change in volume was measured by imaging the oil meniscus level in 613 the capillary tube and then analyzing the images using Blender motion 614 tracking to determine the meniscus position over time. The volume 615 changes were then calculated and normalized by the sample weight. 616 The procedure and data analysis are explained in detail in our 617 previous study. The camera resolution allows the change in height of 618 the oil meniscus to be measured with 0.02 mm accuracy. Combined 619 with the cross-sectional area of the capillary, the corresponding 620 volume change is around 0.0007 mL, whereas typical volume changes 621 in each experiment are roughly 0.05 mL. We believe that the greatest 622 variability in the experiments comes from the fact that mixing may not 623 be perfectly reproducible in such small samples. For example, if a large 624 drop of the mixture becomes entrained in the oil phase early during 625 the experiment, it may crystallize earlier or later than the rest of the 626

Since samples are in liquid—liquid equilibrium prior to crystal- 628 lization, the rate of mixing was found to have a significant effect on the 629 kinetics of crystallization. As such, a rotor assembly was designed and 630 implemented to ensure similar mixing in each sample. The rotor 631 assembly consists of five rotors connected by intermeshed gears and is 632 driven by a single motor that drives the center gear by an elastic band. 633 The motor rotation speed was set to 140 rpm for all experiments.

635 ASSOCIATED CONTENT

636 Data Availability Statement

637 Experimental data, including the evolution of volumes with 638 time, and spreadsheets of the data used to plot Figures 2, 3, 4, 639 and 6 will be available on request.

640 Supporting Information

641 The Supporting Information is available free of charge at 642 https://pubs.acs.org/doi/10.1021/acs.langmuir.3c02428.

Additional experimental data analysis of crystallization kinetics including figures and alternate method of quantifying crystallization kinetics. Also, microscopic images of hydrate melting point, salt crystals (PDF)

647 AUTHOR INFORMATION

648 Corresponding Author

Sachin S. Velankar – Department of Chemical Engineering,
 University of Pittsburgh, Pittsburgh 15261 Pennsylvania,
 USA; Department of Mechanical Engineering, University of
 Pittsburgh, Pittsburgh 15261 Pennsylvania, USA;
 Email: velankar@pitt.edu

654 Authors

661

662

Michael Gresh-Sill – Department of Chemical Engineering,
 University of Pittsburgh, Pittsburgh 15261 Pennsylvania,
 USA

Sudesna Banerjee – Department of Chemical Engineering,
 University of Pittsburgh, Pittsburgh 15261 Pennsylvania,
 USA; orcid.org/0000-0002-9535-405X

Tara Y. Meyer – Department of Chemistry, University of Pittsburgh, Chevron Science Center, Pittsburgh 15260 Pennsylvania, USA

664 Complete contact information is available at:

665 https://pubs.acs.org/10.1021/acs.langmuir.3c02428

666 Author Contributions

667 Michael Gresh-Sill has done the methodology, data curation, 668 writing—original draft preparation; software; validation; formal 669 analysis; and investigation. Sudesna Banerjee is responsible for 670 writing—review and editing. Tara Meyer is responsible for 671 writing—review and editing. Sachin Velankar has done the 672 methodology; supervision; writing—review and editing; and 673 conceptualization.

674 Funding

675 This research was supported by the National Science 676 Foundation Award (CBET 1933037) and the Mascaro Center 677 for Sustainable Innovation at the University of Pittsburgh.

678 Notes

679 The authors declare no competing financial interest.

680 **ACKNOWLEDGMENTS**

681 The authors thank Dr. Hari Sunkara from Dupont for making 682 the POCB available to us, Mr. Dylan Butler and Ms. Maya 683 Roman for assisting with the design of the rotor assembly, and 684 Ms. Emily Barker from the University of Pittsburgh for 685 discussions.

686 REFERENCES

- 687 (1) Tadokoro, H.; Takahashi, Y.; Chatani, Y.; Kakida, H. Structural 688 studies of polyethers, [—(CH2)m—O—]n.V. Polyoxacyclobutane. 689 *Makromol. Chem.* **1967**, *109*, 96–111.
- 690 (2) Banerjee, J.; Koronaios, P.; Morganstein, B.; Geib, S. J.; Enick, R. 691 M.; Keith, J. A.; Beckman, E. J.; Velankar, S. S. Liquids That Freeze

- When Mixed: Cocrystallization and Liquid–Liquid Equilibrium in 692 Polyoxacyclobutane–Water Mixtures. *Macromolecules* **2018**, 51, 693 3176–3183.
- (3) Chatani, Y.; Kobatake, T.; Tadokoro, H. Structural studies of 695 poly(ethylenimine). 3. Structural characterization of anhydrous and 696 hydrous states and crystal structure of the hemihydrate. *Macro-* 697 *molecules* 1983, 16 (2), 199–204.
- (4) Benkhira, A.; Franta, E.; Francois, J. Polydioxolane in aqueous 699 solutions. 1. Phase diagram. *Macromolecules* **1992**, 25 (21), 5697—700 5704.
- (5) Guenet, J.-M. Polymer-Solvent Molecular Compounds; Elsevier, 702 2010 703
- (6) Barker, E.; Banerjee, S.; Meyer, T. Y.; Velankar, S. Liquids that 704 Freeze when Mixed: Homogeneous Cocrystallization Kinetics of 705 Polyoxacyclobutane—Water Hydrate. *ACS Appl. Polym. Mater.* **2022**, 706 4, 703–713.
- (7) Banerjee, S.; Gresh-Sill, M.; Barker, E. F.; Meyer, T. Y.; Velankar, 708 S. S. Polymer co-crystallization from LLE: Crystallization kinetics of 709 POCB hydrate from two-phase mixtures of POCB and water. *Polymer* 710 **2023**, 282, 126087.
- (8) Chido, M. T.; Koronaios, P.; Saravanan, K.; Adams, A. P.; Geib, 712 S. J.; Zhu, Q.; Sunkara, H. B.; Velankar, S. S.; Enick, R. M.; Keith, J. A. 713 Oligomer hydrate crystallization improves carbon nanotube memory. 714 *Chem. Mater.* **2018**, *30*, 3813–3818.
- (9) Badeau, B. A.; DeForest, C. A. Programming stimuli-responsive 716 behavior into biomaterials. *Annu. Rev. Biomed. Eng.* **2019**, 21 (1), 717 241–265.
- (10) Municoy, S.; Álvarez Echazú, M. I.; Antezana, P. E.; 719 Galdopórpora, J. M.; Olivetti, C.; Mebert, A. M.; Foglia, M. L.; 720 Tuttolomondo, M. V.; Alvarez, G. S.; Hardy, J. G. Stimuli-responsive 721 materials for tissue engineering and drug delivery. *Int. J. Mol. Sci.* 722 **2020**, 21, 4724.
- (11) Babu, P.; Nambiar, A.; He, T.; Karimi, I. A.; Lee, J. D.; 724 Englezos, P.; Linga, P. A Review of Clathrate Hydrate Based 725 Desalination To Strengthen Energy—Water Nexus. ACS Sustainable 726 Chem. Eng. 2018, 6, 8093—8107.
- (12) Freier, E.; Wolf, S.; Gerwert, K. Proton transfer via a transient 728 linear water-molecule chain in a membrane protein. *Proc. Natl. Acad.* 729 *Sci. U. S. A.* **2011**, *108* (28), 11435–11439.
- (13) Gadjourova, Z.; Andreev, Y. G.; Tunstall, D. P.; Bruce, P. G. 731 Ionic conductivity in crystalline polymer electrolytes. *Nature* **2001**, 732 412, 520–523.
- (14) Wei, M.; Gao, Y.; Li, X.; Serpe, M. J. Stimuli-responsive 734 polymers and their applications. *Polym. Chem.* **2017**, *8*, 127–143. 735 (15) Albertsson, P.-Å. Aqueous Polymer-Phase Systems. In *Partition* 736
- of Cell Particles and Macromolecules; Wiley: New York, 1986; 8–39 737 (16) Lee, H.-N.; Rosen, B. M.; Fenyvesi, G.; Sunkara, H. B. UCST 738
- and LCST phase behavior of poly(trimethylene ether) glycol in water. 739

 J. Polym. Sci. A Polym. Chem. 2012, 50, 4311–4315. 740
- (17) Liu, Y.; Wang, Y.; Cai, W. Salting Effect of Sodium Hydroxide 741 and Sodium Formate on the Liquid–Liquid Equilibrium of 742 Polyoxymethylene Dimethyl Ethers in Aqueous Solution. *Journal Of* 743 *Chemical & Engineering Data* **2019**, 64 (6), 2578–2592.
- (18) Ananthapadmanabhan, K. P.; Goddard, E. D. Aqueous biphase 745 formation in polyethylene oxide-inorganic salt systems. *Langmuir* 746 **1987**, 3 (1), 25–31.
- (19) Thormann, E. On understanding of the Hofmeister effect: how 748 addition of salt alters the stability of temperature responsive polymers 749 in aqueous solutions. *RSC Adv.* **2012**, *2*, 8297.
- (20) Zafarani-Moattar, M. T.; Sadeghi, R. Measurement and 751 correlation of liquid—liquid equilibria of the aqueous two-phase 752 system polyvinylpyrrolidone—sodium dihydrogen phosphate. Fluid 753 Phase Equilib. 2002, 203 (1), 177—191.
- (21) Zhang, Y.; Furyk, S.; Sagle, L. B.; Cho, Y.; Bergbreiter, D. E.; 755 Cremer, P. S. Effects of Hofmeister Anions on the LCST of PNIPAM 756 as a Function of Molecular Weight. *J. Phys. Chem. C* **2007**, *111*, 757 8916–8924.
- (22) Herbst, J.; Pott, R. W. M. The Effect of Temperature on 759 Different Aqueous Two-Phase Diagrams of Polyethylene Glycol (PEG 760

- 761 6000, PEG 8000, and PEG 10000) + Potassium Sodium Tartrate + 762 Water. *Journal Of Chemical & Engineering Data* **2019**, 64 (7), 3036–763 3043.
- 764 (23) Sosa, F. H. B.; Farias, F. O.; Igarashi-Mafra, L.; Mafra, M. R. 765 Measurement and correlation of aqueous two-phase systems of 766 polyvinylpyrrolidone (PVP) and manganese sulfate: Effects of 767 molecular weight and temperature. *Fluid Phase Equilib.* **2018**, 472, 768 204–211.
- 769 (24) Jana, S.; Uchman, M. Poly(2-oxazoline)-based stimulus-770 responsive (Co)polymers: An overview of their design, solution 771 properties, surface-chemistries and applications. *Prog. Polym. Sci.* 772 **2020**, 106, 101252.
- 773 (25) Zaslavsky, B. Y.; Bagirov, T. O.; Borovskaya, A. A.; Gasanova, 774 G. Z.; Gulaeva, N. D.; Levin, V. Y.; Masimov, A. A.; Mahmudov, A. 775 U.; Mestechkina, N. M.; Miheeva, L. M.; Osipov, N. N.; Rogozhin, S. 776 V. Aqueous biphasic systems formed by nonionic polymers I. Effects 777 of inorganic salts on phase separation. *Colloid. Polymer Sci.* 1986, 264, 778 1066–1071.
- 779 (26) Hyde, A. M.; Zultanski, S. L.; Waldman, J. H.; Zhong, Y.-L.; 780 Shevlin, M.; Peng, F. General Principles and Strategies for Salting-Out 781 Informed by the Hofmeister Series. *Org. Process Res. Dev.* **2017**, *21*, 782 1355–1370.
- 783 (27) Bianchi, E.; Ciferri, A.; Tealdi, A.; Torre, R.; Valenti, B. Bulk 784 Properties of Synthetic Polymer-Inorganic Salt Systems. II. Crystal-785 lization Kinetics of Salted Poly(caproamide). *Macromolecules* **1974**, 7, 786 495–500.
- 787 (28) Valenti, B.; Bianchi, E.; Tealdi, A.; Russo, S.; Ciferri, A. Bulk 788 Properties of Synthetic Polymer-Inorganic Salt Systems. IV. Role of 789 the Polymeric Substrate. *Macromolecules* **1976**, *9*, 117–122.
- 790 (29) Hashifudin, A.; Sim, L. H.; Chan, C. H.; Ramli, H. Phase 791 behaviour and morphology of composite comprising of poly(ethylene 792 oxide), polyacrylate and lithium perchlorate. *Compos. Interfaces* **2014**, 793 21, 797–805.
- 794 (30) Dendy Sloan, E.; Koh, C. A. Chapter 4: Effect of 795 Thermodynamic Inhibitors on Hydrate Formation. In *Clathrate* 796 *Hydrates of Natural Gases*; CRC Press: Boca Raton, FL, 2008; pp 797 229–236
- 798 (31) Florin, E.; Kjellander, R.; Eriksson, J. C. Salt effects on the 799 cloud point of the poly(ethylene oxide)+ water system. *J. Chem. Soc.*, 800 Faraday Trans. 1 1984, 80 (11), 2889.
- 801 (32) Huddleston, J. G.; Willauer, H. D.; Griffin, S. T.; Rogers, R. D. 802 Aqueous Polymeric Solutions as Environmentally Benign Liquid/803 Liquid Extraction Media. *Ind. Eng. Chem. Res.* 1999, 38, 2523–2539. 804 (33) Sadeghi, R.; Jahani, F. Salting-In and Salting-Out of Water-805 Soluble Polymers in Aqueous Salt Solutions. *J. Phys. Chem. B* 2012, 806 116 (17), 5234–5241.
- 807 (34) Kakida, H.; Makino, D.; Chatani, Y.; Kobayashi, M.; Tadokoro, 808 H. Strutural Studies of Polyethers [-(CH2)mO-]n. VIII. Polyox-809 acyclobutane Hydrate (Modification I). *Macromolecules* **1970**, *3*, 810 569–578.
- 811 (35) Simion, A. I.; Grigoras, C.-G.; Rosu, A.-M.; Gavrila, L. 812 Mathematical Modelling of Denisty and Viscosity of NACL Aqueous 813 Solutions. *Journal Of Agroalimentary Porcesses and Technologies* **2014**, 814 21, 41–52.
- 815 (36) Mandelkern, L. Crystallization of Polymers: Kinetics & 816 Mechanism, 2nd ed.; Cambridge University Press: New York, USA, 817 2004; 2, Chapter 9
- 818 (37) Mandelkern, L. Crystallization of Polymers: Kinetics & 819 Mechanism, 2nd ed.; Cambridge University Press: New York, USA, 820 2004; 2, Chapter 11
- 821 (38) Iwamatsu, M. Direct numerical simulation of homogeneous 822 nucleation and growth in a phase-field model using cell dynamics 823 method. *J. Chem. Phys.* **2008**, *128* (8), No. 084504.